polymer

2,3-Dihydroxypropyl methacrylate and 2-hydroxyethyl methacrylate hydrogels: gel structure and transport properties

G. Gates[a], J.P. Harmon[a,*], J. Ors[b], P. Benz[b]

[a]*University of South Florida, 4202 East Fowler Avenue, Tampa, FL 33620, USA*
[b]*Benz Research and Development, P.O. Box 1839, Sarasota, FL 34230, USA*

Abstract

The drying kinetics were examined in four cross-linked polymers that form hydrogels: 2,3-Dihydroxypropyl methacrylate (DHPMA) and 2-hydroxyethyl methacrylate (HEMA) and two random copolymers, with one-to-one and three-to-one HEMA-to-DHPMA molar ratios. The hydrogels were saturated with buffered, isotonic saline solution and deionized water; weight loss kinetics were monitored at temperatures from 16 to 37 °C at 30 and 60% relative humidity under air flow. While there are numerous studies of diffusion in hydrogels, this is one of few studies examining the initial evaporative drying period. The analyses of this short time data revealed that increasing the DHPMA content decreased water volatility; the percent water loss rate decreased with DHPMA content. Long time desorption data coupled with differential scanning calorimetry (DSC) results suggest that departure from Fickian desorption kinetics coincides with the onset of non-freezing water desorption. Dynamic mechanical analysis (DMA) revealed that changes in stiffness accompanying desorption are much more pronounced in HEMA containing polymers. Preliminary results indicate that the ion transport rate is greater in DMPMA containing hydrogels.
© 2002 Elsevier Science Ltd. All rights reserved.

Keywords: Hydrogel; Drying kinetics; Transport kinetics

1. Introduction

A number of years ago homopolymers and copolymers of 2-hydroxyethyl methacrylate (HEMA) and 2,3-dihydroxypropyl methacrylate (DHPMA), and cross-linked with ethylene glycol dimethacrylate were synthesized for use in applications requiring hydrophilic polymers [1]. Recent advances in DHPMA purification techniques awakened interest in these polymers. Since DHPMA has two hydroxyl groups on every repeat unit that interacts with water molecules, compared to only one with HEMA, copolymerization with DHPMA increases equilibrium water content. This feature has generated much interest in their use as contact lens materials and in other biomedical applications. To date research characterizing these polymers is limited. Some initial thermal analysis studies characterized water structure and the effects of water on transitions in these polymers [2,3]. Another group performed some initial NMR studies to further characterize water–polymer interactions [4,5].

There have been no complete studies characterizing transport properties in these polymers. This is important, for example, in contact lens applications because lens parameters such as curvature and diameter change with dehydration, and lens dehydration decreases oxygen transport rates [6]. In hydrogels, desorption processes are complicated; transport depends on both surface evaporation and diffusion through the polymer. The parameters that govern desorption of water from hydrogels may change over time, so models that predict drying behavior are solved using numerical methods with finite differences [7]. The drying process occurs in two phases: the first is evaporation-limited with control of moisture transfer dominated by a combination of capillary flow and liquid volatility; the second is controlled by moisture transfer resulting from thermodynamic coupling of heat and mass transfer processes [8]. Polymer relaxations are an important factor in the late stages of drying due to changes in matrix mobility. However, the initial desorption rate of hydrogels are most significant for contact lens applications.

For the initial drying phase, time $\rightarrow 0$, the loss of penetrant by surface evaporation $(dM/dt)_{t=0}$ (g/s), is

* Corresponding author. Tel.: +1-813-974-3397; fax: +1-813-974-1733.
E-mail address: harmon@chuma1.cas.usf.edu (J.P. Harmon).

proportional to the water surface concentration, C_0, which is independent of the total water content in the hydrogel; linear time dependency is observed according to Eq. (1) [9]:

$$(dM/dt)_{t=0} = KF_0(C_0 - C_{ext}) \tag{1}$$

The concentration immediately above the evaporation surface is C_{ext}, but this quantity becomes negligible if the surrounding air velocity is sufficiently high. The variable, F_0 (g/cm^2 s), represents the evaporation rate of pure water under the experimental conditions, independent of physio-chemical hydrogel and water interaction effects. The moisture transfer coefficient, K, is included to account for the influences on F_0, including capillary and water–matrix associative effects. The product of K and F_0 therefore expresses the volatility of water (g/cm^2 s) within the hydrogel environment at a specific temperature. There is limited research on the initial evaporative drying period, which for contact lens applications is the most significant drying period.

The drying period subsequent to initial evaporation depends on the rate at which water is supplied to the surface by convective processes, specifically, diffusion within the hydrogel bulk [10]. If Fick's law governs the diffusion processes desorption kinetics exhibit square root of time dependency [11]. Sun and Lee have shown, however, that desorption transport mechanisms in hydrogels are not clearly defined [12]. Desorption rates depend on the degree association between the water and the matrix, the greater the association, the easier the water is removed. A classical method of describing transport in polymers is via the power law [7]:

$$M_t/M_\infty = k^*(t)^n \tag{2}$$

The variable t represents time, M_t is the mass of water gained or lost at time t, M_∞ is the initial mass of water contained in the polymer, and n is the diffusion exponent that determines the diffusion mechanism. The transport mechanism is usually described by two limiting cases of this power law model: $n = 0.5$ and $n = 1$. If solvent transport is controlled exclusively by the chemical potential gradient, $n = 0.5$ and little or no dimensional change during transport. This is referred to as Case I or Fickian diffusion, and is described by a diffusion coefficient. If $n = 1$, the rate is proportional to time, and stress relaxation controls kinetics and dimensional changes counteract the mechanical stresses produced by solvent transport [13,14]. This is termed Case II diffusion, and the velocity of the solvent front describes the process. The intermediate case, known as anomalous diffusion, occurs when solvent transport is proportional to time^n, where $0.5 < n < 1$. Transport results from a mixture of Case I and Case II processes, and both solvent-front velocity and diffusion coefficient describe the process [15].

Desorption is affected by the association between water and the polymer matrix, correspondingly influencing the value of the moisture transfer coefficient. This association

has been studied by differential scanning calorimetry and water hydrogels is classified as bound and freezing water, and the bound fraction is further classified as non-freezing water or freezing-bound water. The non-freezing water fraction is composed of water molecules intimately associated with the hydrophilic groups in the polymer matrix, and does not freeze in calorimetric investigations [16–18]. Water molecules independent of the polymer matrix freeze as bulk water. Freezing-bound water has an intermediate association with the polymer matrix and exhibits a crystallization exotherm at lower temperatures, ca. $-40\,°C$, than that observed for free water, ca. $-20\,°C$ [18]. DSC does not detect bound water, but bound water is estimated by extrapolation of a linear plot of enthalpy against water content [18].

This study analyzes the desorption process for water and saline solution in DHPMA and HEMA homopolymers and copolymers. Analysis of the initial drying period is emphasized. Kinetics are interpreted and related to the 'state' of the penetrant as determined via DSC studies. In addition, dynamic mechanical analysis (DMA) is used to characterize physical properties of the matrix that are related to water content, specifically changes in the modulus of the matrix accompanying water loss during desorption. Some initial results on ion transport are also presented.

2. Experimental

2.1. Materials and sample preparation

Four different polymers, supplied as soft contact lens blanks of standard size (12.8 mm diameter, 6.0 mm thick), were manufactured by and obtained from Benz Research and Development Corporation: the HEMA and DHPMA homopolymers, and two HEMA/DHPMA random copolymers. The names and compositions of the copolymers, lot numbers, linear expansion coefficients and the weight-percent water at equilibrium swelling for all the materials in this study are provided in Table 1. All the polymers were synthesized using a patented process (US Patent No. 5,532,289), with water or ethylene glycol used as a diluent during polymerization; the cross-linker concentration was approximately 0.2% by weight EGDMA for all the materials.

Samples 0.50 mm thick were cut from the contact lens blanks using a diamond-wafering blade lubricated with silicone oil, and rinsed in hexane. The samples were oven-dried, at $120\,°C$ under vacuum. The drying time for DHPMA was approximately twice that required by HEMA.

2.2. Differential scanning calorimetry

For DSC analysis, 0.50 mm thick samples were cut from the contact lens blanks using a diamond-wafering blade lubricated with silicone oil. The thin disks were rinsed in

Table 1
Characterization information for materials studied

Polymer name	Molar ratio DHPMA/HEMA	Lot number	Water content swelled to equilibrium at 23 °C (wt%)	Linear expansion coefficient
DHPMA homopolymer	1:0	49002G11 15X	75	1.59
1 DHPMA:1 HEMA copolymer (5X)	1:1	937105G15X	59	1.39
1 DHPMA:3 HEMA copolymer (3X)	1:3	841088G13X	49	1.28
HEMA homopolymer	0:1	802522PMCL	38	1.19

hexane, and then completely hydrated in buffered saline solution consisting of 8.01 g NaCl, 2.47 g H_3BO_3 and 0.14 g $Na_2BO_4 \cdot 10H_2O$ in one L of deionized water (pH = 7.3, 295 milliosmoles). The samples analyzed by DSC were cut from these disks with a #1 cork bore at different times during the desorption process. The samples were quickly weighed to ±0.01 mg, sealed in aluminum hermetic pans, and immediately analyzed by DSC. The sample mass ranged from 5 to 10 mg. Following DSC analysis, the samples were oven dried under vacuum and the dry polymer mass was obtained. The water mass was determined by subtracting the dry mass from the mass of the DSC sample. A Sartorius balance (model BP210D), accurate to ±0.01 mg was used to determine mass. The dry sample mass was recorded after further drying produced no change in the mass.

All calorimetric data were obtained by measuring heat flow with a TA Instruments 2920 differential scanning calorimeter (DSC), calibrated with indium and equipped with a nitrogen purge gas at a flow rate of 60 ml/min. The partially hydrated polymers were analyzed by cooling the samples from 23 to −80 °C at 5 °C/min. All data manipulation was performed using the TA Instruments *Universal Analysis 2.6* program. The water content (W_C) for the partially hydrated samples was reported as the water mass divided by the dry polymer mass. The total integrated area of the crystallization exotherm was plotted against water content. The amount of non-freezing water was determined by the water content intercept of the linear plot.

2.3. Desorption experiments

For the desorption experiments, samples were cut from the contact lens blanks and rinsed in hexane, as described above. Each material was cut according to the linear expansion coefficient so that at equilibrium, all four materials had the same thickness. Prior to desorption analysis, the thin disks were dry polished using 1200 grit emery paper and 1 μm alumina-coated plastic sheets. The disks were subsequently swelled to equilibrium in deionized water or buffered saline solution, and a #7 cork bore was used to cut a 10.5 mm diameter sample from each disk. The samples were dried for 7 days at atmospheric conditions to obtain the dry mass, and then, the samples were returned to solution and allowed to equilibrate for 1-week prior to desorption analysis. The thickness at equilibrium in solution

was 0.70 ± 0.05 mm, measured using a Max-Cal electronic digital caliper, accurate to ±0.05 mm. The diameter to thickness ratio for all the hydrogels in solution was 15:1 at equilibrium.

Desorption experiments were conducted using an IGAsorp Moisture Sorption Analyser, manufactured by Hiden Analytical, housed at R. P. Scherer in St. Petersburg, FL. The mass resolution of the instrument was 0.2 μg. The mass change during desorption was recorded as a function of time using an airflow of 500 ml/min at both 30 and 60% relative humidity. All desorption experiments were conducted at 16, 23, 30, and 37 °C. For the hydrogels saturated in deionized water, only the HEMA and DHPMA homopolymers were compared, but all four polymers (HEMA, 3X, 5X, DHPMA) were compared in buffered saline solution. The mass loss during the first 20 min of desorption was recorded. Additionally, the mass loss of the DHPMA homopolymer, saturated in saline solution, was studied over a 10-h period at 30% relative humidity at all four temperatures; a 3-h desorption period, under the same conditions, was used for the HEMA homopolymer for comparison. For the gravimetric analysis, the samples were removed from solution (maintained at the temperature of interest), blotted dry with filter paper, and placed in a 200 μm mesh basket. The temperature and humidity chamber was then immediately raised to surround the sample, and the balance was tared to mark zero time. The mass was recorded every 10 s for at least 20 min.

2.4. Dynamic mechanical analysis

For the dynamic mechanical analysis, the TA Instruments Dynamic Mechanical Analyzer 2980 was used in the tension mode, and storage modulus was recorded as a function of desorption time. TA Instruments *Thermal Advantage* software was used to operate the instrument, and the program, *Universal Analysis 2.6*, was used for data manipulation. The dimensions of the swollen samples were 12 mm long, 0.35 mm thick (±0.05 mm) and 6 mm wide. These samples were cut from the contact lens blanks, as previously described. The temperature was maintained using the TA Instruments nitrogen gas-cooling accessory (GCA), so that desorption occurred under a nitrogen atmosphere. The frequency of each analysis was 1 Hz, and the amplitude was 5 μm. A preload force of 0.001 N was
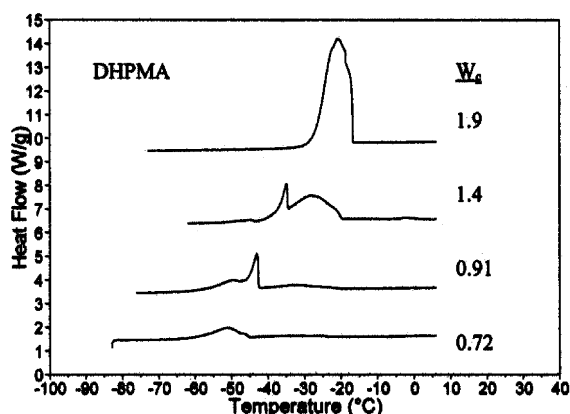
Fig. 1. Cooling curves for the DHPMA homopolymer during desorption of saline, with water content (g water/g dry polymer) indicated at right of curve. Curves have been displaced on the *y*-axis for clarity.

used to maintain sample tension, and the force tracking option was used at 105%.

2.5. Ion-transport

For the ion-transport experiments, actual contact lenses made from HEMA and the 5X copolymer saturated in buffered saline solution were studied; the thickness of the lenses was 0.080 ± 0.005 mm. The experimental apparatus consisted of a chamber containing 3 ml of 1000 ppm Na^+ ions separated from a second chamber containing 3 ml of 1000 ppm K^+ ions, both solutions were Aldrich atomic emission standards in 0.01% HCl solution. The alkali metal solutions were separated by a contact lens, thoroughly rinsed in deionized water, which completely covered a 4.70 mm diameter hole in a ball and socket joint, sealed with a spring clamp. For 10 min, the potassium ion solution diffused into the sodium ion solution, and the sodium ion solution diffused into the potassium ion solution. The solutions were constantly stirred at the same speed using two micro stir-bars that were mounted approximately 5 mm from the base of the contact lens on either side. At the conclusion of the 10-min mixing period, the potassium ion solution was analyzed for sodium ion concentration, and the sodium ion solution was analyzed for potassium ions using inductively coupled plasma (ICP) atomic emission spectroscopy (AES). Analysis was performed using a Vista RL CCD Simultaneous ICP AES, housed at the University of Florida, after calibration at 2 and 10 ppm with the diluted standards previously described. For each solution analyzed, the instrument conducted five replicate analyses and the mean was reported.

3. Results and discussion

3.1. Differential scanning calorimetry
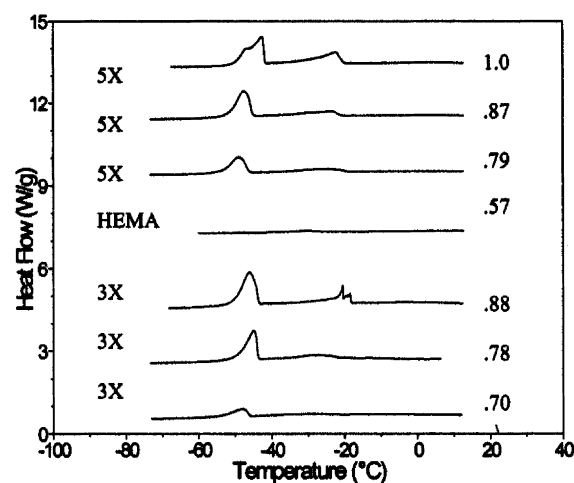
DSC cooling curves were obtained for the DHPMA

Fig. 2. Cooling curves at different states of partial hydration (g water/g dry polymer) for all four hydrogels equilibrated in buffered saline solution. Water contents are indicated at the right of each curve. Curves have been displaced on the *y*-axis for clarity.

homopolymer at different stages of buffered saline desorption. The results shown in Fig. 1 show a single exotherm at ca. $-20\,°C$ at a water content (W_C) equal to 1.9 g water/g dry polymer (65 wt%). The same exotherm is observed at the equilibrium water content of 3.0 g/g. Only freezing water, or water not effected by the polymer matrix, is detected by DSC during initial desorption, almost no detectable change in water structure occurs during early time desorption, from 75 wt% at equilibrium to 65 wt%. Continued desorption of saline results in the appearance of the freezing-bound water exotherm at $-40\,°C$. The freezing-bounds water fraction has an intermediate association with the polymer matrix [18]. Both the freezing water and freezing-bound water exotherms decreased in area and temperature with continued desorption of saline solution, until almost no crystallization was detected at a water content of 0.72 g/g, or 43 wt%. A linear extrapolation of enthalpy against water content defines the water content producing no crystalline enthalpy at 0.72 ± 0.03 g/g.

The DSC cooling curves for two HEMA–DHPMA copolymers, 5X and 3X, during desorption of saline are similar, as shown in Fig. 2. The integrated area of the free water and freezing-bound water crystallization exotherms is slightly greater for the 5X copolymer during the initial stages of desorption. In both copolymers, the integrated area of the lower temperature exotherm, indicating freezing-bound water, is greater that the higher temperature exotherm during the initial stages of desorption. During desorption, the exotherms decreased in temperature and area. A linear extrapolation of enthalpy against water content defines the water content producing no crystallization enthalpy at $0.65 \pm$ g/g in the 3X and 5X copolymers.

Cooling curves were obtained for HEMA homopolymer at equilibrium in buffered saline solution, as shown in Fig. 2. The data show a very small exotherm at $-20\,°C$, but no reproducible analysis of the crystallization exotherm

integrated area as a function of saline content was achieved during desorption. Therefore, the majority of water in HEMA is intimately associated with the polymer matrix, existing as non-freezing water, approximately 35 wt% bound water as compared to 38 wt% water at equilibrium. These data agree with the previous DSC and NMR analyses of HEMA in saline that determined bound water content at 30 ± 5 wt% [17]. Given that the amount of freezing water in HEMA was so much less than observed in DHPMA polymers, transport rates were examined to see if significant differences exist, as observed in other hydrogels [19].

3.2. Desorption

The weight loss data normalized to original water content, or percent weight loss for the DHPMA homopolymer (M_t/M_∞) at 16 and 37 °C are shown in Fig. 3 as a function of the square root of time. The material was initially saturated with isotonic saline and desorbed to dryness at 30% relative humidity; the HEMA homopolymer is included for comparison. There is an initial period with near-zero slope during which surface evaporation dominates desorption. This is followed by a rectilinear interval dominated by diffusion. Finally, an asymptotic region develops at very low moisture content, for DHPMA at about (M_t/M_∞) > 0.8 and for HEMA at about (M_t/M_∞) > 0.6. Interestingly, the water content in DHPMA that produced no crystallization exotherm, 0.72 g/g or 41 wt% water, coincides with the start of the asymptotic desorption region at approximately 75% total desorption. In HEMA, the start of the asymptotic region coincides with slightly greater than 60% total water desorption, even though virtually no crystallization exotherm is detected in saturated HEMA.

The initial weight loss, at t < 5 min, is proportional to time, and (M_t/M_∞) is plotted against time in Fig. 4, for the initial desorption of buffered, isotonic saline from all four hydrogels at 30 °C and 60% relative humidity. If these data were not normalized to the original water content, the four plots would be virtually indistinguishable. However, it is important to emphasize that in the early stages of drying,
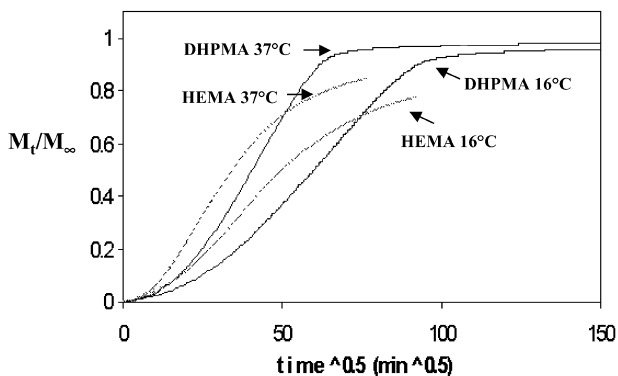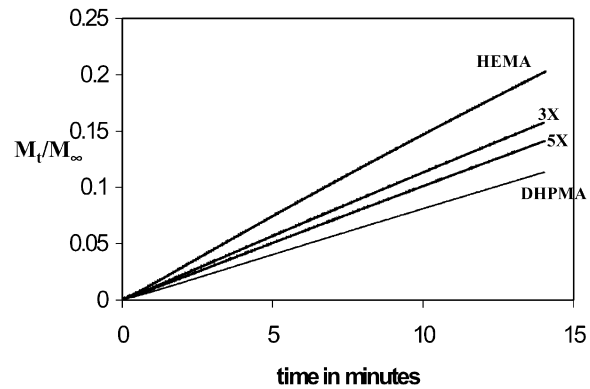

Fig. 4. Initial drying data for the HEMA and DHPMA homopolymers and the 1 DHPMA:3 HEMA copolymer (3X) and the 1 DHPMA:1 HEMA copolymer (5X) initially saturated with isotonic saline, desorbing at 60% relative humidity and 30 °C.

boundary layer phenomena controlled the process of drying through evaporation, independent of the original water content (M_∞); in the latter stages of drying, internal diffusion resistance of water through the polymer dominates desorption and dependence on M_∞ must be considered [20].

Using Eq. (1), the weight loss during the initial five minutes of desorption, shown in Figs. 5 and 6, is used to determine the volatility of water in the hydrogel. The volatility of water depends on the four temperatures studied, the surrounding air velocity (which was maintained constant at 500 ml/min), and the water surface area. The water surface area is obtained by subtracting the surface area of the dry disk (determined using the expansion coefficient in Table 1) from the surface area of the swollen disk. In Eq. (1), the concentration of water vapor above the disk, C_{ext}, was negligible using the vapor pressure of water at 30 and 60% relative humidity; the high air velocity also contributed to the justified negligibility of C_{ext} [9]. The evaporation rate or the volatility of water from the hydrogels is proportional to the difference in the concentration of water on the surface and the concentration of water immediately above the surface. Therefore, the water volatility in these hydrogels was determined by normalizing
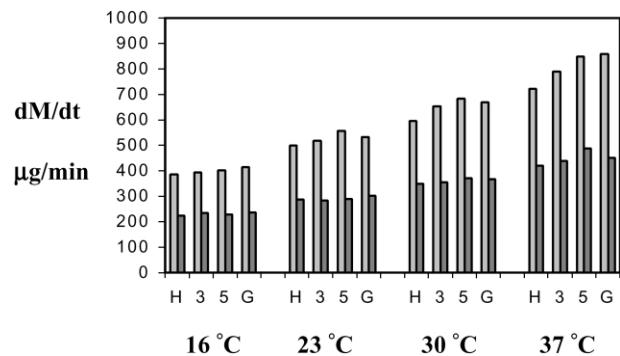

Fig. 3. Percent weight loss for the HEMA and DHPMA homopolymers in initially saturated with isotonic saline at 30% relative humidity.

Fig. 5. The mass loss (dM/dt)$_{t=0-5 \text{ min}}$, $r^2 > 0.9995$, for the hydrogels at 30% relative humidity (grey) and at 60% relative humidity (black), as a function of temperature, for the initial five minute desorption of buffered, isotonic saline solution.
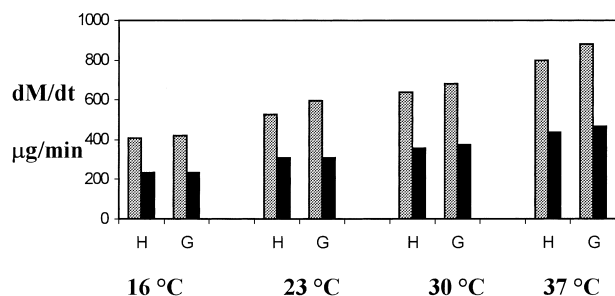
Fig. 6. The mass loss $(dM/dt)_{t=0-5\ min}$, $r^2 > 0.9995$, for the HEMA and DHPMA homopolymers at 30% relative humidity (grey) and at 60% relative humidity (black), as a function of temperature, for the initial 5-min desorption of deionized water.

the weight-loss data in Figs. 5 and 6 to the water surface area; the results are expressed in Tables 2 and 3.

In all instances, the volatility is greater in the hydrogels saturated with deionized water, compared to the isotonic saline-saturated hydrogels. This is attributed to a decrease in the ion-osmotic swelling pressure with an increase in ionic strength [21]. Increasing the DHPMA content in the hydrogels decreases the volatility, or the initial desorption flux, even though the weight loss during the first 5 min, or $(dM/dt)_t = 0-5$ min, increases with DHPMA content. The lower volatility in DHPMA is attributed to the greater surface area of water, due to the increased expansion coefficient as DHPMA content increases. Higher relative humidity decreases volatility, as would be expected because of the reduced chemical potential gradient.

For this investigation, the primary objective was to determine if the initial desorption rate of water from HEMA hydrogels is different from that observed in DHPMA hydrogels. Since DHPMA has two hydroxyl groups per repeat unit, compared to only one in HEMA, it is hypothesized that the increased hydroxyl content per unit volume in the DHPMA dry polymer will slow the initial evaporation process; this phenomenon is observed in the data shown in Table 3. However, acting in consort with the polarity contributions are the effects of sub-micron size: smaller size water surfaces, as expected in HEMA, evaporate with greater ease due to higher vapour pressure, compared to larger sizes, as expected in DHPMA [22]. To illustrate, the enthalpy of vaporization for bulk water at 25 °C is approximately $+10.5$ kcal/mol [23]. As the size of

the evaporating water surface decreases to the sub-micron range, the vapour pressure increases, corresponding to increased evaporation rate; the minimum enthalpy for liquid water is 1.78 kcal/mol, the total surface energy per mole of liquid water [24].

Therefore, the activation energy of the initial evaporation rate observed in these hydrogels was determined using the Arrhenius dependence of the volatility (Tables 2 and 3) on the absolute temperature, with the results presented in Table 4. The activation energy ranges from 5.2 to 6.2 kcal/mol, and the HEMA homopolymers are consistently the lowest, corresponding to the highest observed evaporation rate. It does not appear to be possible, using these desorption data, to attribute the depressed evaporation rates in the DHPMA hydrogels to either sub-micron size effects or polarity effects separately, given that all of these hydrogels were synthesized using the same cross-link concentration and diluent concentration during polymerization. At high temperature and low humidity, however, the decreased evaporation rate correlates to increased water surface area with $r^2 > 0.990$, but the correlation decreases to $r^2 > 0.960$ at high humidity and low temperature.

The diffusivity is calculated from the diffusion control portion of the curves in Fig. 3 using the following equation [11]:

$$M_t/M_\infty = (4/L)(Dt\pi^{-1})^{0.5}, \quad M_t/M_\infty < 0.5 \qquad (3)$$

For desorption, the variable t represents desorption time (s), M_t is the mass of water desorbed at time t, M_∞ is the initial mass of water contained in the polymer, $2L$ is the thickness of the plane sheet (cm), and D is the diffusivity (cm²/s). The

Table 2
The volatility of water ($KF_0 \times 10^6$ g/cm² s) $r^2 > 0.9990$, for the hydrogels at 30% relative humidity, as a function of temperature, for the initial 5-min desorption of isotonic saline solution and deionized water

Temperature (°C)	Saline				Water	
	DHPMA	5X	3X	HEMA	DHPMA	HEMA
16	5.26	6.77	8.50	11.4	5.35	12.0
23	6.77	9.38	11.2	14.7	7.56	15.5
30	8.52	11.5	14.1	17.6	8.66	18.9
37	10.99	14.3	17.0	21.44	11.2	23.6

Table 3
The volatility of water ($KF_0 \times 10^6$ g/cm² s) $r^2 > 0.9990$, for the hydrogels at 60% relative humidity, as a function of temperature, for the initial 5-min desorption of isotonic saline solution and deionized water

Temperature (°C)	Saline				Water	
	DHPMA	5X	3X	HEMA	DHPMA	HEMA
16	3.00	3.85	5.05	6.65	2.96	6.89
23	3.88	4.87	6.12	8.51	3.93	9.07
30	4.66	6.25	7.68	10.3	4.77	10.5
37	5.74	7.53	9.47	12.4	5.92	12.8

Table 4
The volatility of water activation energy for HEMA and DHPMA saturated with deionized water, and for HEMA, 3X, 5X, and DHPMA saturated with buffered saline solution, $r^2 > 0.990$

Polymer name	Activation energy in water (kcal/mol)		Activation energy in saline (kcal/mol)	
	30%	60%	30%	60%
HEMA	5.64	5.26	5.27	5.26
3X			5.88	5.36
5X			6.21	5.74
DHPMA	6.20	5.78	6.13	5.41

diffusion coefficient, D, is an apparent diffusion coefficient, since concentration dependency and water-polymer interactions contribute to the water flux.

Results for the HEMA and DHPMA homopolymers desorbing isotonic saline solution at 30% relative humidity and all four temperatures are presented in Table 5. The reported diffusivity data for HEMA agrees with desorption literature data, 2×10^7 cm^2/s [15]. The Arrhenius dependence of diffusivity on temperature yields the apparent activation energy for HEMA (6.36 kcal/mol) that is less than DHPMA (7.40 ± 0.05 kcal/mol) for both $0.2 < (M_t/M_\infty) < 0.4$ and for $0.4 < (M_t/M_\infty) < 0.6$.

3.3. Dynamic mechanical analysis

The stiffness of the HEMA and DHPMA hydrogels was examined during desorption of deionized water and buffered saline in a nitrogen atmosphere. Two temperatures were used, 23 and 37 °C; the results from the 23 °C desorption of buffered saline are shown in Fig. 7; analogous results are obtained from the 37 °C experiments. There is no significant difference between samples equilibrated in water or in buffered saline solution.

The HEMA storage modulus at zero time in water and in saline is greater than the DHPMA homopolymer because there is initially twice as much water in the DHPMA homopolymer or one-half the number of polymeric chains per unit volume; the modulus results for HEMA are similar to previous studies [1]. The stiffness increases as the materials desorbed, and this is greater in HEMA than in the DHPMA materials. In fact, the DHPMA homopolymer does not show a detectable change in stiffness until the sample desorbed for 15 min; the HEMA homopolymer immediately evidences increased stiffness upon desorption.

3.4. Ion-transport

An ion-transport study was conducted to access whether differences exist between the Na$^+$ and K$^+$ ion diffusion rates in HEMA compared to the 5X copolymer. These ions were reported to have similar transport rates across a HEMA membrane, and have comparable hydrodynamic radii [21]. The actual contact lenses that were used in this study were received at equilibrium in buffered saline solution, and thoroughly rinsed prior to use in the study. However,
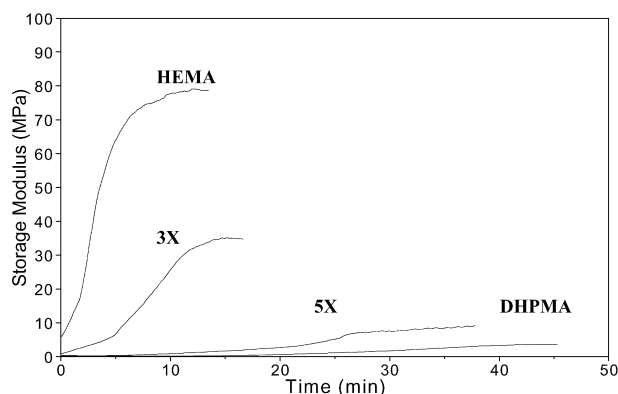

Fig. 7. The modulus during drying of the hydrogels at 23 °C, initially saturated with isotonic, buffered saline solution.

sodium ions could have been trapped in the hydrogel matrix, so that the sodium ion data could not be considered as reliable as the potassium ion transport data. For the six ion-transport experiments conducted, equal volumes and dilute concentrations (1000 ppm) of pure monovalent ions, obtained as spectroscopic standards, were used.

Generally, the diffusivity of a solute through a physically cross-linked membrane increases as the volume fraction of water within the gel increases [25]. Therefore, the ion concentrations using the 5X copolymer membrane are expected to be greater. The results, summarized in Table 6, indicate that after the 10-min diffusion period, the potassium ion concentration in the sodium solution is approximately six times greater for the 5X copolymer, compared to the HEMA homopolymer. The sodium ion concentration in the potassium solution is also greater for the 5X copolymer, but it was less precise compared to the potassium ion results. Although the non-freezing water fractions, estimated using DSC, are virtually the same in these two hydrogels, the ion transport rate in the 5X copolymer is clearly greater, since this material has greater water content, 59-wt% in the 5X copolymer compared to 38-wt% in HEMA.

4. Conclusions

The DSC analysis shows that in saline solution, HEMA homopolymer and the two HEMA–DHPMA copolymers have virtually the same non-freezing water content, but that of DHPMA homopolymer is greater. Although there is no

Table 5
The desorption diffusion coefficient of water ($D \times 10^7$ cm^2/s), $r^2 > 0.995$, at 30% relative humidity, as a function of temperature, for the hydrogels initially saturated with isotonic saline

Temperature (°C)	HEMA $0.2 < (M_t/M_\infty) < 0.4$	DHPMA $0.2 < (M_t/M_\infty) < 0.4$	DHPMA $0.4 < (M_t/M_\infty) < 0.6$
16	1.51	1.28	1.53
23	2.03	1.79	2.23
30	2.58	2.40	2.90
37	3.22	3.06	3.69

Table 6
Results from ICP atomic emission spectroscopy ion transport experiments conducted with contact lenses made from HEMA and 5X copolymer

Lens material	Ion concentration (ppm)	
	Na^+	K^+
HEMA	2.01	0.877
HEMA	3.21	1.12
HEMA	2.13	1.10
5X	5.72	6.37
5X	6.76	6.32
5X	7.13	6.60

freezing water detected by DSC in HEMA, copolymerization with DHPMA increases freezing water content. The DHPMA homopolymer desorbs almost 10% of the original water content before DSC analysis detects any change in water structure. The DSC analysis is not sufficiently sensitive to detect differences in water structure between deionized water and buffered saline equilibration. Since the partially desorbed samples used for DSC were not allowed any equilibration time prior to analyses, the water structure in the thermograms is correlated to the gravimetric water desorption analysis. The long time desorption data for DHPMA, coupled with DSC results, suggest that as freezing water desorbs linearly with the square root of time, departure from linearity coincides with non-freezing water desorption. The gravimetric desorption experiments demonstrate that although the absolute rate of water loss in DHPMA is greater than that observed in HEMA, the percent water loss rate decreased at the DHPMA content increased. The apparent activation energy of desorption was much more pronounced in HEMA than in DHPMA containing polymers. In fact, significant desorption occurred in the DHPMA homopolymer before any change in stiffness was detected. Finally, the rate of ion transport was greater in the 5X copolymer compared to the HEMA homopolymer.

References

[1] Refojo MJ. J Appl Polym Sci 1965;9:3161–70.
[2] Gates GA, Harmon J, Ors J, Benz PA. ANTEC. Proceedings of the 59th Annual Technical Conference and Exhibition, May 6, vol. XLVII. Dallas, TX: Society of Plastics Engineers; 2001. p. 1891.
[3] Gates GA, Harmon J, Ors J, Benz PA. Polymer in press.
[4] McConville P, Pope JM. Polymer 2001;42:3559–68.
[5] McConville P, Pope JM. Polymer 2000;41:9081–8.
[6] Brennan N, Lowe R, Efron N, Ungerer L, Carney L. Am J Optom Physiol Optic 1987;64(7):534–9.
[7] Astarita G. In: Mashelkar R, editor. Transport phenomena in polymeric systems. New York: Wiley; 1989. p. 339–51.
[8] Shukla KN. In: Hsieh RKT, editor. Series in Theoretical and Applied Mechanics. Singapore: World Scientific; 1990.
[9] Vergnaud JM. Liquid transport processes in polymeric materials. Englewood Cliffs, NJ: Prentice-Hall; 1991. p. 14.
[10] Frisch HL. J Polym Sci: Part B: Polym Phys 1978;16:1651–64.
[11] Crank J, Park GS. Diffusion in polymers. London: Academic Press; 1968. p. 16–25.
[12] Sun YM, Lee HL. Polymer 1996;37(17):3915–9.
[13] Harmon JP, Lee S, Li JCM. J Polym Sci: Polym Chem. 1987;25: 3215–29.
[14] Harmon JP, Lee S, Li JCM. Polymer 1988;29:1221–6.
[15] Chou KF, Han CC, Lee S. Polym Engng Sci 2000;40(4):1004–14.
[16] Barbieri R, Quaglia M, Delfini M, Brosio E. Polymer 1998;39(5): 1059–66.
[17] Quinn FX, Kampff E, Smyth G, McBriety VJ. Macromolecules 1988; 21(11):3191–204.
[18] Hatakeyama H, Hatakeyama T. Thermochim. Acta 1998;308(1–2): 3–22.
[19] Murphy SM, Hamilton CJ, Davies ML, Tighe BJ. Biomaterials 1992; 13(14):979–90.
[20] Messadi D, Vergnaud J, Hivert M. J Appl Polym Sci 1981;26:667–77.
[21] Khare AR, Peppas NA. Polymer 1993;34(22):4736–9.
[22] Atkins P. Physical chemistry, 4th ed. New York: Freeman; 1990. p. 147.
[23] Mahan B. University chemistry, 3rd ed. Reading, MA: Addison-Wesley; 1975. p. 137.
[24] Adamson AW. Physical chemistry of surfaces, 2nd ed. New York: Interscience; 1967. p. 57.
[25] Murphy SM, Hamilton CJ, Tighe BJ. Polymer 1988;29:1887–93.